AIAA-95-1488-C

FLUTTER ANALYSIS OF COMPOSITE WINGS USING AN EXACT DYNAMIC STIFFNESS MATRIX METHOD

G.A.Georghiades*, S.J.Guo** and J.R. Banerjee***

Department of Mechanical Engineering and Aeronautics

City University

Northampton Square

LONDON EC1V OHB, U.K.

Abstract

An analytical investigation has been carried out into the aeroelastic behaviour of composite wings using an exact dynamic stiffness matrix method. Emphasis is given on how the fiber orientation affects the stiffness and coupling parameters of a composite wing (unswept and swept), and in turn, how these parameters affect the flutter speed. Results are presented for three different but related wing configurations. The significances of results are discussed.

Introduction

It is well known that composite materials display anisotropic behaviour and exhibit coupling between various modes of structural deformation[1-8]. As a consequence of this anisotropic property, the stiffnesses of a composite structure can be controlled in a beneficial way leading to, for example, structural optimization and/or aeroelastic tailoring of aircraft wings[9-14]. In this paper, an analytical investigation has been carried out into the aeroelastic behaviour of composite wings using an exact dynamic stiffness matrix method. (This paper appears to be the first to use an exact dynamic stiffness formulation in the flutter analysis of composite wings.) The effect of stiffness parameters on flutter speed of graphite/epoxy cantilevered wings is investigated for various ply orientations and sweep angles.

* Research Student
** Research Fellow
*** Senior Lecturer

Of particular interest to which this work is addressed, is the inclusion of the coupling stiffness between the bending and twisting modes of structural deformation in the flutter analysis. Such coupling is notably prevalent in composite wings but is non-existent in metallic ones. The investigation is mainly focused on the flutter behaviour of swept-back composite wings. The desired stiffness and/or coupling parameters are achieved by varying the fiber orientation of the laminae from which the wing is made. The main contribution made in this paper is the use of the dynamic stiffness matrix method in the flutter analysis of a high aspect ratio composite wing. (The wing is considered to be essentially an assembly of composite beams.) Numerical results are obtained for various cases but the emphasis is given on how the fiber orientation affects the stiffness and coupling parameters of a composite wing, and in turn, how these parameters affect the flutter speed. The effect of sweep is also taken into account in the analysis.

Using the dynamic stiffness matrix method[15] the free vibration characteristics of a composite wing are first established (some advantages of the dynamic stiffness matrix method in free vibration analysis are well known[16], particularly when higher frequencies and better accuracies are required. The method often forms a useful comparator to finite element and other approximate methods). The flutter speed is then computed using a computer program in FORTRAN, called **CALFUN**[17] (**CA**lculation of **F**lutter speed **U**sing **N**ormal modes), which uses generalized coordinates and normal modes (obtained from the dynamic stiffness method) to calculate the flutter speed of a cantilever aircraft wing from its basic

structural and aerodynamic data. The normal mode method of flutter analysis used in **CALFUN** is well established and has been reported in a number of papers[18-20]. Basically the method relies on the fact that the dynamic stiffness (which includes mass and inertia) and aerodynamic properties of an aircraft wing can be expressed in terms of the generalized coordinates. Thus, following this procedure, **CALFUN** calculates the natural frequencies and normal modes of an aircraft wing and then obtains its generalized dynamic stiffness and aerodynamic matrices, respectively. The flutter matrix is formed by algebraically summing the generalized dynamic stiffness and aerodynamic matrices. It is then solved for flutter speed and flutter frequency using both an exact method and the well known V-g method[21].

Composite Beam Rigidities

The rigidity properties of a composite beam are derived from the classical theory of anisotropic plates and lamination theory[22-23]. The procedure is briefly summarised as follows.

The relationship between plate bending moments, twisting moment, and curvatures of the midsurface of a plate can be expressed[22] as:

$$\begin{Bmatrix} M_x \\ M_y \\ M_{xy} \end{Bmatrix} = \begin{bmatrix} D_{11} & D_{12} & D_{16} \\ D_{12} & D_{22} & D_{26} \\ D_{16} & D_{26} & D_{66} \end{bmatrix} \begin{Bmatrix} k_x \\ k_y \\ k_{xy} \end{Bmatrix} \quad (1)$$

where the elements D_{ij} are the flexural modulus components of a laminated composite plate which depend on both the fiber orientation and the stacking sequence of the individual plies in the laminate.

Thus following the procedure described in Ref.22, the elements D_{ij} for an n-ply laminate with arbitrary ply angle orientation are given in the usual notation as follows:

$$D_{ij} = \sum_{k=1}^{n} Q_{ij}^{\beta k} \left[z_k^3 - z_{k-1}^3 \right] / 3 \quad (2)$$

$$i, j = 1, 2, 6$$

where $Q_{ij}^{\beta k}$ is the off-axis lamina modulus of the kth ply with an angle of orientation β_k, and z_k is the vertical distance from the midplane to the upper surface of the kth ply.

The effective bending, torsional and coupling rigidities (stiffnesses) of a slender composite beam (i.e. EI, GJ and K respectively) can be expressed in terms of the above plate properties as follows (see, for example, Ref.13):

$$EI = b\left[D_{22} - \frac{D_{12}^2}{D_{11}} \right] \quad (3)$$

$$GJ = 4b\left[D_{66} - \frac{D_{16}^2}{D_{11}} \right] \quad (4)$$

$$K = 2b\left[D_{26} - \frac{D_{12} D_{16}}{D_{11}} \right] \quad (5)$$

where b is the width of the plate.

The non-dimensionalised cross-coupling parameter φ which is a measure of the coupling between the bending and twisting modes of deformation is defined as[13]:

$$\varphi = \frac{K}{\sqrt{EIGJ}} \quad (6)$$

The rigidity properties derived above are now used in the following section to establish the dynamic stiffness properties of a composite beam.

Dynamic Stiffness Matrix Method

An exact dynamic stiffness matrix of a composite beam has recently been derived by Banerjee and Williams[15]. Following the same method (and same notation wherever possible) the natural frequencies and mode shapes of a composite beam (wing) are calculated as follows.

The coupled bending-torsional beam theory for free natural vibration of a thin-walled composite beam as shown in Fig.1 with shear deformation, rotary inertia and warping stiffness neglected, is governed by the following differential equations[15]

$$EIh''' + K\psi'' + m\ddot{h} = 0 \qquad (7)$$

$$GJ\psi'' + Kh''' - I_\alpha \ddot{\psi} = 0 \qquad (8)$$

where h and ψ are respectively, the bending and torsional displacements, m is the mass per unit length, I_α is the polar mass moment of inertia per unit length about the Y-axis, and primes and dots denote differentiation with respect to position y and time t, respectively.

If a sinusoidal variation of h and ψ, with circular frequency ω, is assumed, then

$$\left.\begin{aligned} h(y,t) &= H(y)\sin\omega t \\ \psi(y,t) &= \Psi(y)\sin\omega t \end{aligned}\right\} \qquad (9)$$

where $H(y)$ and $\Psi(y)$ are the amplitudes of the sinusoidally varying bending displacement and torsional rotation respectively.

Substituting equations (9) into equations (7) and (8), the general solution for $H(y)$ and $\Psi(y)$ can be obtained in terms of six arbitrary constants[15], A_i (i = 1,2,...6). Then using the end conditions for bending displacement $H(y)$, bending rotation $\Theta(y)$ ($=H'(y)$) and twist $\Psi(\xi)$ for end 1 and end 2 of the beam (see Fig.2), the following matrix relationship can be obtained (see Ref.15).

$$\{U\} = [B]\{A\} \qquad (10)$$

where

$\{U\} = \{H_1 \quad \Theta_1 \quad \Psi_1 \quad H_2 \quad \Theta_2 \quad \Psi_2\}^T$ is the displacement vector,

$\{A\} = \{A_1 \quad A_2 \quad A_3 \quad A_4 \quad A_5 \quad A_6\}^T$ is the constant vector, $[B]$ is a 6x6 frequency dependant matrix related to the end conditions for displacements, and the upper suffix T denotes a transpose.

Similarly by introducing end conditions for forces (i.e. shear force $S(y)$, bending moment $M(y)$ and torque $T(y)$) into Eqn.(10) the nodal forces can be expressed in terms of the constants A_i (i = 1,2,...6) in matrix form as follows

$$\{F\} = [D]\{A\} \qquad (11)$$

where $\{F\} = \{S_1, M_1, T_1, S_2, M_2, T_2\}^T$ and $[D]$ is a frequency dependant 6x6 matrix related to the end conditions for forces (see Fig.2).

Eqn.(10) can be arrange in the form

$$\{A\} = [B]^{-1}\{U\} \qquad (12)$$

By introducing Eqn.(12) into Eqn.(11), the relationship between the nodal forces and displacements can be obtained as

$$\{F\} = [B]^{-1}[D]\{U\} = [K_D]\{U\} \qquad (13)$$

where

$$[K_D] = [D][B]^{-1} \qquad (14)$$

is the required dynamic stiffness matrix relating harmonically varying forces and displacements at the nodes (ends) of the beam element.

Once the dynamic stiffness matrix is known, the calculation of natural frequencies and mode shapes follows from the well established algorithm of Wittrick and Williams[24] which has received wide attention in recent years[25].

Flutter Analysis Using CALFUN

CALFUN is a computer program in FORTRAN which uses the normal mode method and generalised coordinates to compute the flutter speed of a high aspect ratio aircraft wing from its basis structural and aerodynamic data[17] . The normal mode method of flutter analysis used in **CALFUN** is well established and has been reported in a number of papers[18-20]. Basically the method relies on the fact that the dynamic stiffness properties (i.e. the frequency dependent combined mass and stiffness properties) and aerodynamic properties of an aircraft wing can be expressed in terms of the generalised coordinates. First **CALFUN** calculates the natural frequencies and normal modes of an aircraft wing and then obtains its generalised dynamic stiffness and aerodynamic matrices, respectively. The flutter matrix is then formed by algebraically summing the generalised dynamic stiffness and aerodynamic matrices.

In the structural idealisation of the wing, beam and lumped mass elements are used in **CALFUN** to obtain the dynamic stiffness $[K_D]$ of the wing. The natural frequencies ω_i and the normal mode shapes ϕ_i (where i is the order of the natural frequency /normal mode) are then calculated using the Wittrick-Williams algorithm[24-25].

The generalised dynamic stiffness matrix $[K_G]$ is obtained by diagonalising the dynamic stiffness matrix with the help of the above mode shapes and making use of the orthogonality condition of the normal mode shapes. The generalised aerodynamic matrix $[QF]$ is calculated by using the strip theory and the principle of virtual work[20-21]. Next, the flutter determinant is formed as follows.

The flutter determinant is the determinant formed from the flutter matrix, and the flutter matrix is formed by algebraically summing the generalised dynamic stiffness and aerodynamic matrices. Thus for a system without structural damping (structural damping has generally a small effect on the oscillatory motion and is not considered here) the flutter matrix $[QA]$ can be formed as

$$[QA]\{q\} = \{[K_G] - [QF]\}\{q\} \qquad (15)$$

For the flutter condition to occur, the determinant of the complex flutter matrix must be zero so that from equation (15)

$$\left|[K_G] - [QF]\right| = 0 \qquad (16)$$

The solution of the above flutter determinant is a complex double eigenvalue problem because the determinant is primarily a complex function of two unknown variables, the airspeed (V) and the frequency (ω) . The method normally used in **CALFUN**[18] selects an airspeed and evaluates the real and imaginary parts of flutter determinant for a range of frequencies. The process is repeated for a range of airspeeds until both the real and imaginary part of the flutter determinant (and hence the whole flutter determinant) vanish completely. (**CALFUN** also uses an alternative approach employing the well known V-g method to check the flutter speed.

Results

Prior to the flutter analysis, the rigidity (stiffness) parameters of a uniform composite wing are obtained by classical lamination theory as applied to thin walled composite beams and plates (see egns.(3)-(5)). The wing is represented by a laminated beam (plate) as shown in Fig.1. Then flutter analysis is carried out for three different, but related wing configurations. In the first case, all the fibers of the laminate are assumed to be oriented along a common direction, denoted by the angle β in degrees (i.e. β is same for each ply for this case). This case was chosen so as to give the wing a very high coupling stiffness (K) and relatively low torsional stiffness (GJ). This results into a very strong cross-coupling parameter φ, (see eqn.6), which is a measure of the coupling between the bending and twisting modes of structural deformation. Positive fiber angle (β) gives positive coupling stiffness (K) which in turn gives positive coupling-parameter φ, i.e. a positive (upward) bending displacement causes nose-down twist (see Fig.1). In the second case, 14% of the plies are assumed to be unidirectional i.e. β=0, 28% are oriented symmetrically at β=±45 (of which 14% at β=+45 and 14% at β=-45%), while the remaining 58% of the plies have an orientation β. Thus for instance, the stacking sequence (code/notation) of a laminate with fourteen plies for this case will be $(0/\pm45/\beta/\beta/\beta/\beta)_s$. The reason for choosing this case was that the laminate results in a higher torsional stiffness (GJ) but a lower coupling stiffness (K), with the bending stiffness (EI) very little altered giving an average cross-coupling parameter φ. In the third case, the laminate is balanced and the plies are oriented successively at ±β giving the uncoupled case (i.e. the cross-coupling parameter φ=0). The variations of the non-dimensional bending stiffness (EI/EI_0), torsional stiffness (GJ/GJ_0), the (dimensional) coupling stiffness (K) and the non-dimensional cross-coupling parameter (φ) against the ply orientation β, for the three cases are shown in Fig.3,4 & 5 respectively. In these figures, EI_0 and GJ_0 are the bending and torsional stiffnesses corresponding to the fiber orientation of 0° for each of the plies in the laminate. (Note that the coupling stiffness K has not been non-dimensionalized because K=0 when the fiber

orientation of all plies in the laminate is zero (i.e. K_0=0)). Clearly for the case 3, K = φ = 0. Note that in Figs.3, 4 and 5, the unit of K used is N-m^2.

First the natural frequencies and modes shapes from the present analysis are validated by comparing them with results published in the literature[26]. The illustrative example of the Graphite/Epoxy cantilever beam given in Table 3 of Ref.26 is used for this purpose. The results obtained using the present theory and those of Ref.26 are shown in Table 1. As can be seen, the agreement between the set of results is quite satisfactory.

Based on the rigidity variations shown in Fig.3,4 & 5, the flutter speed of the composite wing is computed for the three cases. The non-dimensionalized flutter speed ratio V_f/V_{f0} where V_f is the flutter speed of the laminated wing for a given stacking sequence (i.e. one of the above three cases) and V_{f0} is the corresponding flutter speed when the fiber orientation in each of the plies in the laminate representing the wing, is set to zero. The investigation is carried out for both swept (backward sweep) and unswept wings. The variation of V_f/V_{f0} against the fiber angle is shown in Figs.6, 7 & 8 for the three cases with the sweep-back angle varying from 0° to 40°. For case 1 it can be seen from Figs.3 & 6 that for all sweep angles the maximum flutter speed occurs when the fiber angle β is somewhere between the maximum torsional rigidity (GJ) and the minimum coupling stiffness (K). The variation of flutter speed is quite pronounced in this case, particularly for negative fiber angles (i.e. negative coupling) giving much higher flutter speed than positive fiber angles. In contrast the results for case 2 (see Figs.4 & 7) show a relatively marginal variation in flutter speed, the maximum occurring again at a fiber angle somewhere between the maximum value of GJ and minimum value of K. The effect of cross-coupling parameter is not so pronounced in this case . The results shown in Figs.5 & 8 are for case 3 in which both K and φ are zero. The results clearly indicate that the maximum flutter speed for the unswept composite wing can be obtained when the plies are alternatively at angles ±45° which gives the maximum possible torsional rigidity (GJ). Interestingly, the maximum achievable flutter speed for the unswept wing of case 3, shown in Fig.8, is much higher than the corresponding (unswept) flutter speeds shown in Figs.6 & 7. The reason for this can be attributed to the fact that the torsional rigidity (GJ) plays a relatively larger role in the flutter of the type of composite wings investigated.

The effect of sweep-back angle is quite pronounced for all the three cases as can be seen from Figs.6, 7 & 8. However, the flutter speed increases with the angle of sweep only for case 1 and 2 in which the coupling parameters K and φ have significant values. These results are in contrast to those of case 3 (see Fig.8) for which no predictable pattern seems to be apparent. However, for case 1 and 2 the effect of sweep angle is most pronounced in the region of maximum value of torsional rigidity GJ and minimum coupling rigidity K. The effect of sweep for the uncoupled case (K=0, i.e. case 3) described in Figs.5 & 8 is very different from the other two cases. It is worth noting that for case 3, the maximum flutter speed for a swept wing does not occur at the maximum torsional rigidity (GJ) (i.e. when the plies are alternatively at angles ±45°) which was the case for the unswept wing. Furthermore as the angle of sweep increases, the maximum flutter occurs at a reduced fiber orientation (i.e. at less than 45°). The departure (reduction) from the original fiber orientation of 45° for the unswept case becomes quite pronounced when the angle of sweep increases to its maximum value. In can be generally observed from Figs.(3)-(8) that a combination of high (GJ) and high negative coupling parameter (φ) with high angle of sweep maximizes the flutter speed. However, it should be noted that GJ and φ are inversely proportional to each other (see egn.6), and also the rigidities EI, GJ and K are not all independent. Therefore a delicate balance is needed to achieve a maximum flutter speed.

Conclusions

The following conclusions are drawn from the above analysis:

1. The cross-coupling parameter (φ) is a very important parameter to be considered when designing a swept-back composite wing from the flutter standpoint. This parameter should preferably be negative i.e. the laminate should, in general, be symmetric but

unbalanced, having more number of plies with negative fiber angles (β) than positive ones.

2. In general, when coupling is present, the maximum flutter speed occurs in the region of maximum torsional rigidity GJ and minimum coupling rigidity K. The investigation has shown that if coupling parameter is present, the fiber angles between -20° and -40° appear to be most effective to give a maximum flutter speed.

3. Sweeping the wing back (aft) from 0° to 40° increases the flutter speed for the case when coupling is present (case 1 and case 2 of the paper). However, when the coupling parameter is non-existent (case 3 of the paper) this is not the case; the flutter speed fluctuates with sweep angles.

4. When the coupling parameter K=0 (case 3 of a paper), the maximum flutter speed of an unswept wing occurs at the maximum torsional rigidity (GJ) (i.e.. the plies are alternatively at angles ±45° for the wing investigated). The flutter speed of the swept wing for this configuration with K=0, occurs at fiber angles lower than 45° and this angle gets further reduced as the angle of sweep is gradually increased.

References

1. Arian, A. A., "Free Vibration Analysis of Anisotropic Thin-Walled Closed-Section Beams," *Proceedings of the 35th AIAA/ASME/ASCE/AHS/ASC Structures, Structural Dynamics, and Material Conference*, Part 5, 1994, pp.164-171.

2. Hodges, D. H., Atilgan, A. R., Fulton, M. V., and Rehfield, L. W., "Free-Vibration Analysis of Composite Beams," *Journal of the American Helicopter Society*, Vol.36, 1991, pp.36-47.

3. Chandra, R., Stemple, D. A., Chopra, I., "Thin-Walled Composite Beams Under Bending, Torsional, and Extensional Loads," *Journal of Aircraft*, Vol.27, No. 7, 1990, pp.619-626.

4. Smith, E. C., and Chopra, I., "Formulation and Evaluation of an Analytical Model for Composite Box-Beams," *Journal of the American Helicopter society*, Vol.36, 1991, pp.23-35.

5. Jensen, W. D., Crawley, F. E., Dugundji, J. "Vibration of Cantilevered Graphite/Epoxy Plates With Bending-Torsion Coupling," *Journal of Reinforced Plastics and Composites*, Vol.1, 1982, pp.254-269.

6. Weisshaar, A. T., Ryan, J. R., "Control of Aeroelastic Instabilities Through Stiffness Cross-Coupling," *Journal of Aircraft*, Vol.23, No.2, 1986, pp.148-155.

7. Weisshaar, T. A., "Divergence of Forward Swept Composite Wings," *Journal of Aircraft*, Vol.17, 1979, pp.442-448.

8. Lottati, I., "Flutter and Divergence Aeroelastic Characteristics for Composite Forward Swept Cantilevered wing," *Journal of Aircraft*, Vol.22, No.11, 1985, pp.1001-1007.

9. Krone, N. J. Jr., "Divergence Elimination With Advanced Composites," *AIAA*, Paper 75-1009, 1975.

10. Shirk, H. M., Weisshaar, A. T., "Aeroelastic Tailoring-Theory, Practice, and Promise," *Journal of Aircraft*, Vol.23, 1986, pp.6-18.

11. Weisshaar, A. T., "Aeroelastic Tailoring of Forward Swept Composite Wings," *Journal of Aircraft*, Vol.18, No.8, 1981, pp.669-676.

12. Austin, F., Hadcock, R., Hutchings, D., Sharp, D., Tang, S., Waters, C., "Aeroelastic Tailoring of Advanced Composite Lifting Surfaces in Preliminary Design," *Proceedings of 17th AIAA/ASME/SAE Structures, Structural Dynamics and Materials Conference*, 1976, pp.69-79.

13. Weisshaar, T. A., and Foist, B. L., "Vibration Tailoring of Advanced Composite Lifting Surfaces," *Journal of Aircraft*, Vol.22, 1985, pp.141-147.

14. Sherrer, C. V., Hertz, J. T., Shirk, H. M., "Wind Tunnel Demonstration of Aeroelastic Tailoring Applied to Forward Swept Wings," *Journal of Aircraft*, Vol.18, No.11, 1981, pp.976-983.

15. Banerjee, J. R., Williams, F. W., "Free Vibration of Composite Beams - An Exact Method Using Symbolic Computation," *Journal of Aircraft* (accepted for publication).

16. Banerjee, J. R., Williams, F. W., "Coupled Bending-Torsional Dynamic Stiffness Matrix of an Axially Loaded Timoshenko Beam Element," *Int. Journal of Solids Structures*, Vol.31, No.6, 1994, pp.749-762.

17. Banerjee, J. R., "Use and Capability of CALFUN - A Program for Calculation of Flutter Speed Using Normal Modes," *Proc. Int. AMSE Conf. on Modelling & Simulation*, Vol.27-29, Athens, Greece, June 1984, pp.121-131.

18. Banerjee, J. R., "Flutter Characteristics of High Aspect Ratio Tailless Aircraft," *Journal of Aircraft*, Vol.21, 1984, pp.733-736.

19. Banerjee, J. R., "Flutter Modes of High Aspect Ratio Tailless Aircraft," *Journal of Aircraft*, Vol.25, 1988, pp.473-476.

20. Loaring, S. J., "Use of Generalised Co-ordinates in Flutter Analysis," *SAE Journal*, Vol.52, April 1944, pp.113-132.

21. Bisplinghoff, B. L., Ashley, H., and Halfman, R. L., "Aeroelasticity," *Addison-Wesley*, Reading, Massachusetts, 1955.

22. Tsai, W. S., Hahn, T. H., "Introduction to Composite Materials," *Technomic Publishing Company*, Westport, 1980.

23. Datoo, H. M., "Mechanics of Fibrous Composites," *Elsevier Applied Science*, U.S.A, 1991.

24. Wittrick, W. H., Williams, W. F., "A General Algorithm for Computing Natural Frequencies of Elastic Structures," *Q. J. Mech. App. Math.*, 24(3), 1971, pp.263-284.

25. Williams, W. F., "Review of Exact Buckling and Frequency Calculations with Optional Multi-Level Substructuring," *Journal of Computers and Structures*, 48(3), 1993, pp.547-552.

26. Teboub, Y., and Hajela, P., "Free Vibration of Generally Layered Composite Beams Using Symbolic Computations,"*Proceedings of the 35thAIAA/ASME/ASCE/AHS/ASC Structures, Structural Dynamics, and Material Conference*, Paper 94-1330, 1994, pp.182-192.

Table 1: Natural Frequencies (HZ) of a Graphite-Epoxy cantilever beam.

	$\beta = 15^{\circ}$				$\beta = 30^{\circ}$			
Mode No	Refer. [26]	Exptl [26]	Present	Error %	Refer. [26]	Exptl [26]	Present	Error %
1	85.4	82.5	82.1	0.46	52.7	52.7	52.6	0.19
2	531.5	511.3	511.3	0.00	329.8	331.8	328.8	0.90
3	1472.2	1423.4	1413.8	0.67	921.7	924.7	917.4	0.79
4	———	1526.9	———	———	1801.4	1766.9	1783.9	0.96
5	2839.1	2783.6	2743.6	1.44	———	1827.5	———	———
6	3630	4364.6	4403.8	0.90	2967.7	2984	2938.2	1.53
7	4613.4	4731.6	5284.7	11.70	4424	4432.4	4351	1.84

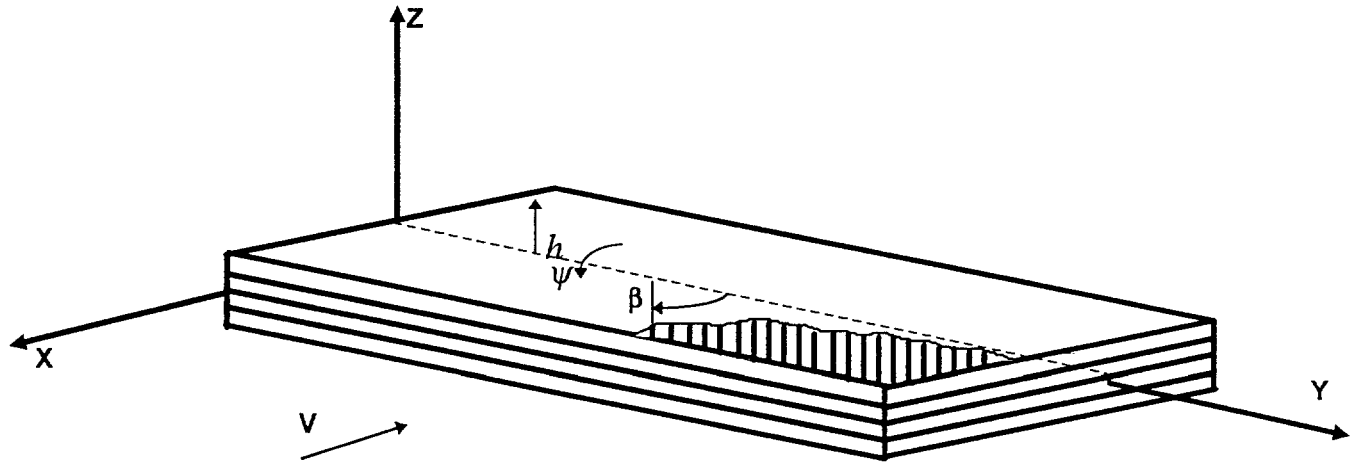

Fig.1. Coordinate system and sign convention for positive ply angle of a laminated composite beam.

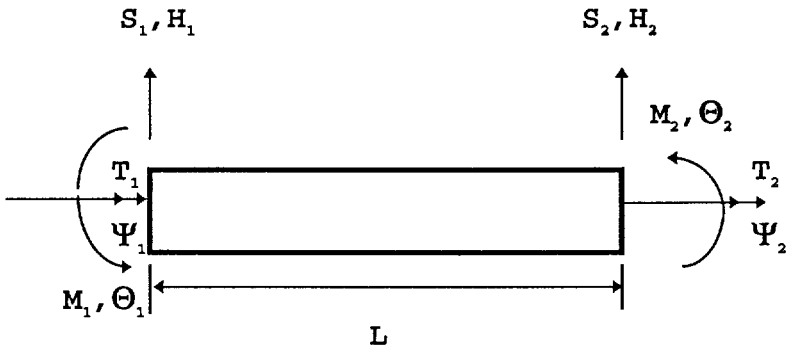

Fig.2. End Conditions for forces and displacements of the beam element.

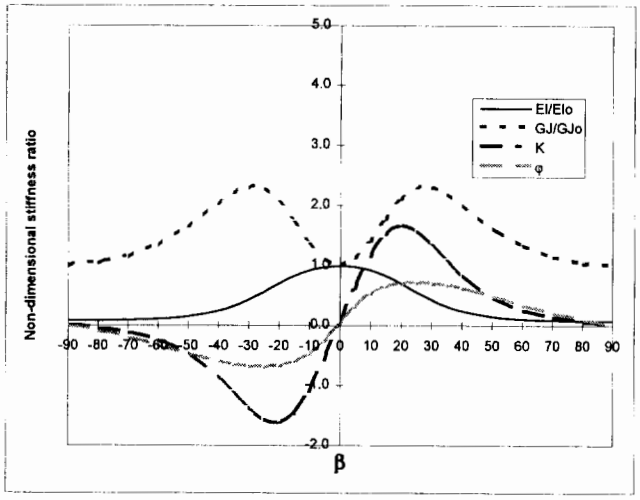

Fig.3. Variation of coupling parameter and bending, torsional and coupling stiffnesses with fiber angle β for case 1 $[\beta]_{14}$.

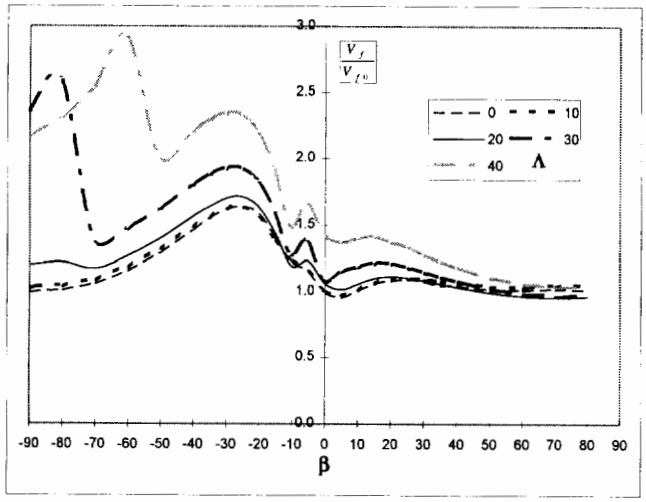

Fig.6. Variation of flutter speed with fiber angle β for various sweep-angles Λ for case 1 $[\beta]_{14}$.

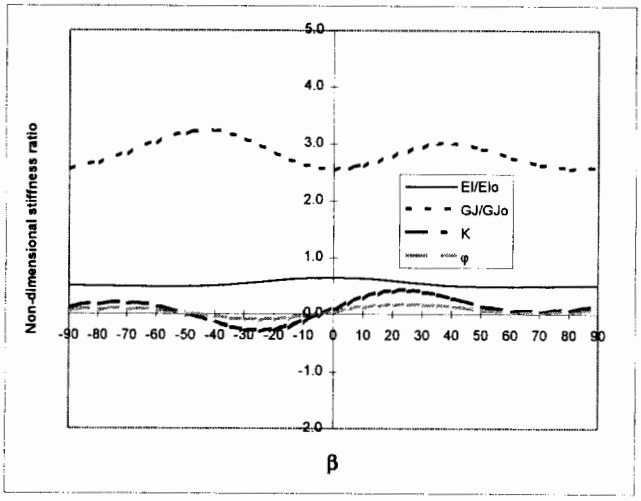

Fig.4. Variation of coupling parameter and bending, torsional and coupling stiffnesses with fiber angle β for case 2 $[0/\pm45/\beta/\beta/\beta]_s$.

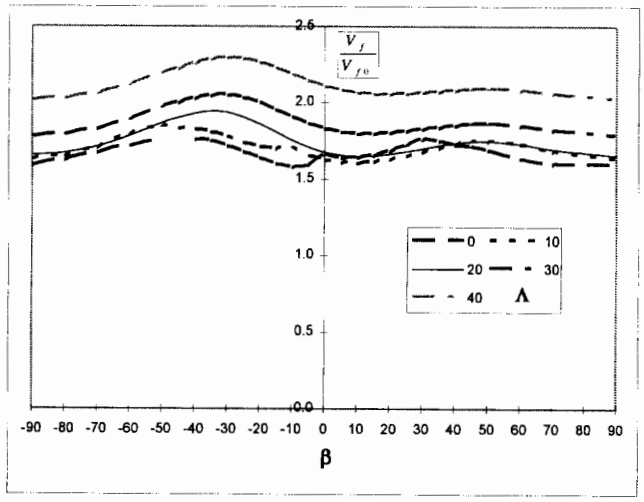

Fig.7. Variation of flutter speed with fiber angle β for various sweep-angles Λ for case 2 $[0/\pm45/\beta/\beta/\beta]_s$.

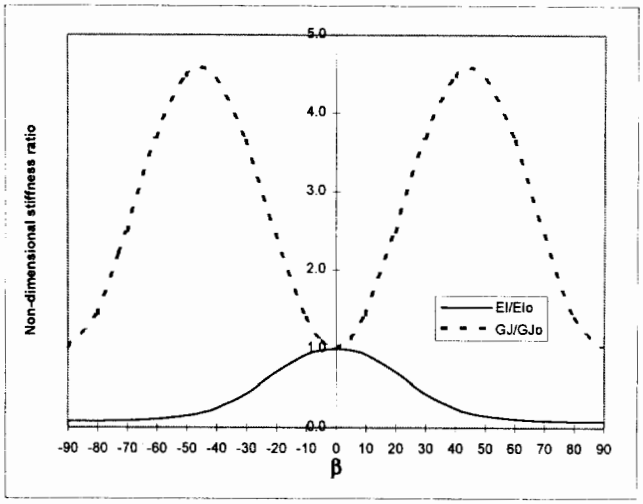

Fig.5. Variation of coupling parameter and bending, torsional and coupling stiffnesses with fiber angle β for case 3 $[\pm\beta]_7$.

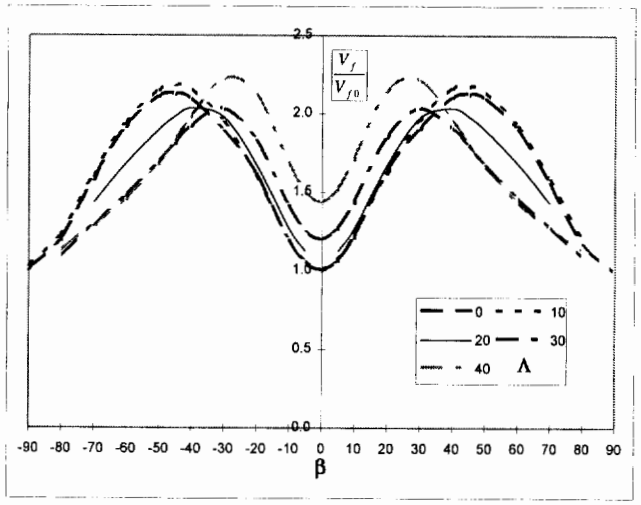

Fig.8. Variation of flutter speed with fiber angle β for various sweep-angles Λ for case 3 $[\pm\beta]_7$.